

Disconnect between Fibrotic Response and Right Ventricular Dysfunction

Slaven Crnkovic^{1*}, Bakytbek Egemnazarov^{1*}, Rachel Damico², Leigh M. Marsh¹, Bence M. Nagy¹, Philipp Douschan^{1,3}, Kwame Atsina⁴, Todd M. Kolb², Stephen C. Mathai², Jody E. Hooper⁵, Bahil Ghanim^{1,6}, Walter Klepetko⁶, Friedrich Fruhwald⁷, Dirk Lassner⁸, Andrea Olschewski¹, Horst Olschewski³, Paul M. Hassoun², and Grazyna Kwapiszewska^{1,9}

¹Ludwig Boltzmann Institute for Lung Vascular Research, Graz, Austria; ²Division of Pulmonary and Critical Care Medicine and ⁵Department of Pathology, Johns Hopkins, Baltimore, Maryland; ³Division of Pulmonology, ⁷Division of Cardiology, and ⁹Otto Loewi Center, Physiology, Medical University of Graz, Graz, Austria; ⁴Division of Cardiology, University of California, Davis, Davis, California; ⁶Department of Thoracic Surgery, Medical University of Vienna, Vienna, Austria; and ⁸Institute for Cardiac Diagnostic and Therapy, Berlin, Germany

ORCID ID: 0000-0002-0820-3318 (S.C.).

Abstract

Rationale: Remodeling and fibrosis of the right ventricle (RV) may cause RV dysfunction and poor survival in patients with pulmonary hypertension.

Objectives: To investigate the consequences of RV fibrosis modulation and the accompanying cellular changes on RV function.

Methods: Expression of fibrotic markers was assessed in the RV of patients with pulmonary hypertension, the murine pulmonary artery banding, and rat monocrotaline and Sugden5416/hypoxia models. Invasive hemodynamic and echocardiographic assessment was performed on galectin-3 knockout or inhibitor-treated mice.

Measurements and Main Results: Established fibrosis was characterized by marked expression of galectin-3 and an enhanced number of proliferating RV fibroblasts. Galectin-3 genetic and pharmacologic inhibition or antifibrotic treatment with pirfenidone

significantly diminished RV fibrosis progression in the pulmonary artery banding model, without improving RV functional parameters. RV fibrotic regions were populated with mesenchymal cells coexpressing vimentin and PDGFR α (platelet-derived growth factor receptor- α), but generally lacked α SMA (α -smooth muscle actin) positivity. Serum levels of galectin-3 were increased in patients with idiopathic pulmonary arterial hypertension but did not correlate with cardiac function. No changes of galectin-3 expression were observed in the lungs.

Conclusions: We identified extrapulmonary galectin-3 as an important mediator that drives RV fibrosis in pulmonary hypertension through the expansion of PDGFR α /vimentin-expressing cardiac fibroblasts. However, interventions effectively targeting fibrosis lack significant beneficial effects on RV function.

Keywords: right ventricle fibrosis; right ventricular function; PDGFR α ; galectin-3

Right ventricle (RV) function determines the outcome in patients suffering from pulmonary arterial hypertension (PAH) (1) and continues to deteriorate in some

patients with PAH despite optimized therapy and improvement in pulmonary resistance (2). The progressive pulmonary vascular disease increases vascular

resistance and initiates a remodeling process in the RV (3), which initially compensates for the increased afterload, but later becomes maladaptive and ultimately

(Received in original form September 21, 2018; accepted in final form December 14, 2018)

*These authors contributed equally to this work.

Supported by the Austrian National Bank Fund (ÖNB Anniversary Fund, #16187, G.K.), Austrian Science Fund (FWF, #P27848, G.K.), and NIH/NHLBI (R01HL132153, R.D. and P.M.H.).

Author Contributions: Study design and manuscript drafting, S.C., B.E., H.O., and G.K. Data acquisition and analysis, S.C., B.E., R.D., L.M.M., B.M.N., P.D., K.A., T.M.K., S.C.M., J.E.H., B.G., W.K., F.F., and D.L. Data interpretation, manuscript revision, and final approval, L.M.M., A.O., H.O., P.M.H., and G.K.

Correspondence and requests for reprints should be addressed to Horst Olschewski, M.D., Medical University of Graz, Ludwig Boltzmann Institute for Lung Vascular Research, Auenbruggerplatz 15, 8036 Graz, Austria. E-mail: horst.olschewski@medunigraz.at.

This article has an online supplement, which is accessible from this issue's table of contents at www.atsjournals.org.

Am J Respir Crit Care Med Vol 199, Iss 12, pp 1550–1560, Jun 15, 2019

Copyright © 2019 by the American Thoracic Society

Originally Published in Press as DOI: 10.1164/rccm.201809-1737OC on December 17, 2018

Internet address: www.atsjournals.org

At a Glance Commentary

Scientific Knowledge on the

Subject: Right ventricular (RV) fibrosis has been linked to RV functional impairment, yet the underlying molecular mechanisms and functional consequences of RV fibrosis have been understudied.

What This Study Adds to the

Field: We identified a major molecular mechanism responsible for expansion of cardiac fibroblasts and development of RV fibrosis. Genetic and pharmacologic reduction of RV fibrosis did not improve cardiac function. Moreover, level of RV fibrosis did not correlate with clinical parameters in patients with idiopathic pulmonary arterial hypertension. Our study cumulatively demonstrates that management of RV dysfunction requires treatments going beyond exclusive antifibrotic activity.

leads to RV failure (4). Investigations into mechanisms of RV remodeling have become a translational necessity, yet most of the studies have focused on changes in RV cardiomyocyte function (5, 6), whereas the composition and function of other resident cells and extracellular matrix have been understudied (7).

Ventricular fibrosis, evident as fibroblast accumulation and extracellular matrix deposition, may cause increased ventricular stiffness (5) and arrhythmia (8). However, the functional significance of RV fibrosis is still unclear. Moreover, the cellular origins and molecular mechanisms governing the fibrosis are still poorly defined. The current understanding centers on the activation of cardiac fibroblasts by profibrotic factors: TGF β (transforming growth factor- β), endothelin-1, and PDGF (platelet-derived growth factor) (9). The final outcome is excessive deposition of fibrillar collagens and other extracellular matrix proteins, proliferation of fibroblasts and their phenotypic change, such as acquisition of α SMA (α -smooth muscle actin) expression (9). This basic paradigm has been expanded to include the deleterious role of inflammation (4). Galectin-3, a profibrotic lectin released by inflammatory cells, was linked to the

development of left ventricle (LV) failure and mortality (10, 11), and RV dysfunction in patients with PAH (12, 13).

Data from the LV indicate that the expansion of resident cardiac fibroblasts and their collagen production is responsible for pressure overload-induced fibrosis (14–16). However, adult cardiac fibroblasts represent a mosaic progeny arising from different lineages (17), hampering the identification of a robust and general marker that could identify all subpopulations and distinguish the cardiac fibroblasts from other nonmyocyte cells. Recent lineage tracing and single cell approaches from the LV have identified PDGFR α (PDGF receptor- α) as a marker of collagen-producing cells potentially including cardiac fibroblasts (14–16, 18).

In the current study, we addressed the cellular and molecular mechanisms governing RV fibrosis by comparative use of animal and human tissue material. Moreover, we sought to determine the functional significance of RV fibrosis by *in vivo* phenotyping of the murine model and antifibrotic approaches using genetic and pharmacologic tools.

Some of the results of these studies have been previously reported as abstracts (19, 20).

Methods

Human Material

RV myocardial autopsies from patients with end-stage PAH (idiopathic PAH [IPAH] and systemic sclerosis PAH [SSc-PAH]) were collected at the Division of Pulmonary and Critical Care Medicine, Johns Hopkins, Baltimore, Maryland (NA00036610). Explant lungs from patients with IPAH and nontransplanted donor lung samples were obtained from the Medical University of Vienna following written consent and approval by the local ethics board according to the declaration of Helsinki (976/2010). Clinical data and serum samples from patients with IPAH and donor control subjects were collected at Graz, Austria (derivation cohort, $n = 10$) after informed written consent and approval by the Medical University of Graz ethics committee (23-408ex10/11). Additionally, validation cohorts of patients with IPAH ($n = 38$) and SSc-PAH ($n = 43$) were identified and analyzed in Baltimore, after approval by the Johns Hopkins University

Institutional Review Board, and informed consent was obtained for all patients (NA000027124, NA00005740). Patient characteristics are provided in Tables E1 and E2 in the online supplement.

Murine Pulmonary Artery Banding Model

Animal experiments were approved by the Austrian Ministry of Education, Science and Culture. Wild-type C56BL/6J mice were obtained from Charles Rivers Laboratories, galectin-3 homozygous knockout mice were obtained from Jackson Laboratories. The pulmonary artery banding (PAB) mouse model was performed as described previously (21). Briefly, mice were anesthetized and mechanically ventilated. An incision was made in the second left intercostal space using sterile technique, the pericardium was removed, and a partially occlusive titanium clip was placed around the main pulmonary artery (Weck). The pulmonary artery was occluded to 0.3 mm, which corresponds to approximately 75% occlusion of the luminal diameter. The mice were then sutured and received postoperative analgesic therapy. Sham-treated animals underwent the same procedure with a vascular clip placed next to the vessel. A Vevo 770 high-resolution imaging system with a 30-MHz RMV-707B scan head (FujiFilm VisualSonics) was used for transthoracic echocardiographic measurements. Investigations were performed under mild anesthesia with isoflurane as described previously (21). For inhibitor studies, at Day 7 postoperation, level of occlusion was checked by echocardiography and mice were randomized to treatment or control group. *N*-Acetyllactosamine (NaCLac), galectin-3 inhibitor (22), was given intraperitoneally 5 mg/kg/d three times per week for a total duration of 3 weeks. Pirfenidone (Toronto Research Chemicals) was mixed with normal chow diet at 2.8 g/kg (ssniff Spezialdiäten) and provided *ad libitum* to mice. Amount of pirfenidone in the food was adjusted to account for average food consumption of 3.5 ± 0.5 g/mouse/d, giving the average daily pirfenidone intake of 400 mg/kg. Actual food consumption was controlled in regular intervals. Invasive hemodynamic measurements were performed under isoflurane anesthesia (1–2%) using a closed-chest technique and a 1.4F pressure catheter (SPR-671, Millar Instruments) as described previously (21).

Pulmonary hypertension in rats was induced by a single subcutaneous application of the VEGFR inhibitor Sugen5416 (20 mg/kg, dissolved in 10% DMSO, 0.9% NaCl, 0.4% Tween, 0.9% benzylalcohol, and 0.5% carboxymethylcellulose) in 220–250 g male rats and exposure for 3 weeks to normobaric hypoxia (10% oxygen), followed by additional 3 weeks of normoxia. Additionally, the monocrotaline rat model was performed according to published reports (23). Briefly, male Sprague-Dawley rats (Janvier) weighing 300 g were injected with a single intraperitoneal injection of monocrotaline (60 mg/kg) or saline followed by organ collection 28 days postmonocrotaline application.

Histological Staining

RV fibrosis was assessed using semiautomated image analysis on Sirius red–stained tissue cuts as described previously (21). Immunohistochemical and immunofluorescent localization of vimentin, PDGFR α , α SMA, and galectin-3 in mouse and human heart or lung tissue is described in the online supplement. A list of used antibodies is provided in Table E4.

ELISA Measurements

Circulating levels of human galectin-3 were determined using commercially available ELISA kit (R&D Systems) in both patient cohorts.

Gene and Protein Expression Analysis

Quantification of gene and protein expression was performed using real-time PCR and Western blotting, respectively, according to protocol in the online supplement. The primer sequences are given in Table E5.

Statistical Analysis

Statistical analysis was performed in GraphPad Prism 5 using an unpaired Student's *t* test, one-way ANOVA with Dunnett *post hoc* test or two-way ANOVA with Bonferroni *post hoc* test, where appropriate. Serum levels of galectin-3 were normalized using *z*-transformation. Correlation analysis was performed using nonparametric Spearman test. *P* less than 0.05 was considered statistically significant.

Results

Cellular Characterization of RV Fibrosis

The cellular composition of RV fibrotic regions is currently unknown. Because of

scarcity of human RV tissue samples, we analyzed the localization of major mesenchymal markers in experimental models displaying RV fibrosis. In three different models of RV remodeling (mouse PAB, rat Sugen5416/hypoxia, and monocrotaline) RV fibrosis was characterized by vimentin and PDGFR α immunoreactivity (Figure 1A). Surprisingly, we rarely observed the myofibroblast marker α SMA immunoreactivity in the corresponding fibrotic regions (Figure 1A). The overlap of vimentin and PDGFR α signal in murine RV was further confirmed by double immunofluorescent staining, whereas costaining with α SMA was generally absent (see Figure E1). Western blotting confirmed these changes with increased levels of PDGFR α , but not α SMA (Figure 1B). Additionally, we observed prominent localization of galectin-3, a profibrotic marker, in the RV from diseased animals (Figures 1C; see Figure E2A) and its increased protein levels (Figures 1D; see Figure E2B). In contrast to the PAB, monocrotaline, and Sugen models, in the RV of chronic hypoxia-exposed mice, a model that does not develop RV fibrosis (24), expression of galectin-3 was unaltered (see Figures E2C and E2D). Galectin-3-positive cells colocalized partially with vimentin⁺ and PDGFR α ⁺ cells (see Figure E2E).

We next investigated whether extensive vimentin⁺/PDGFR α ⁺ staining is caused by a proliferative response or just upregulated expression of the receptors and spreading of existing cardiac fibroblasts. *In vivo* pulse-labeling of proliferating cells with the thymidine analog EdU at Day 3 after PAB traced the presence of EdU⁺ cells at the 3 weeks' time point in vimentin/PDGFR α /galectin-3 immunoreactive regions, but showed no colocalization with α SMA (Figure 1E).

RV Functional Parameters Are Not Causally Related to RV Fibrosis

We next addressed the effects of targeted antifibrotic approaches. Genetic deletion, or pharmacologic inhibition of galectin-3 (NaLac inhibitor) starting at Day 7, a time point at which fibrosis is already present in the RV (25) (Figure 2A), significantly blunted the RV fibrosis development (Figures 2B and 2C; see Figure E3A) and was associated with lesser vimentin, PDGFR α , and galectin-3 immunoreactivity

compared with vehicle-treated mice (Figures 2D and 2E). NaLac-treated and galectin-3 homozygous knockout mice PAB mice were still able to develop RV hypertrophy (Figure 2F; see Figure E3B), but showed no significant change in any of the hemodynamic and echocardiographic parameters (Figures 2G–2K; see Tables E6 and E7). Furthermore, galectin-3 homozygous knockout mice and NaLac-treated mice did not display further significant decrease in capillary density as compared with wild-type/vehicle control animals (see Figures E3C and E3D).

To investigate if these findings could be recapitulated using a pharmacologic approach, we tested the antifibrotic agent pirfenidone, clinically approved for treatment of idiopathic pulmonary fibrosis (Figure 3A). Pirfenidone significantly decreased pressure overload-induced RV fibrosis (Figures 3B and 3C). Pirfenidone also reduced the extent of vimentin, PDGFR α , and galectin-3 immunoreactivity (Figures 3D and 3E), while maintaining the same level of hypertrophic response (Figure 3F). Similar to galectin-3 inhibition, pirfenidone-treated mice showed no significant changes in functional hemodynamic parameters versus vehicle-treated mice (Figures 3G–3K; see Table E8).

We found no or weak correlations between RV fibrosis and hemodynamic and echocardiographic impairment in the diverse subsets of experiments (see Figures E4A–E4F and E5A–E5I). To improve the power of detection of associations, we pooled the data of all experiments. As expected there was a weak but significant correlation between RV fibrosis score and catheter-derived RV end-diastolic pressure and echo-derived tricuspid annular plane systolic excursion (Figures 4A and 4B), and cardiac output (see Figure E5J) but not with RV isovolumetric relaxation constant (τ) (see Figure E4G) or RV relaxation velocity (e') (see Figure E5K). Because most of the effects of antifibrotic treatment on RV function were not significant, we also pooled the data from all subgroups to improve the power to detect more subtle effects of antifibrotic treatment on RV function. In the pooled data set, the treatments had a strong effect on the fibrosis levels; however, the RV functional parameters were unchanged (Figure 4C). This points toward disconnect between RV fibrosis and dysfunction (Figure 4C).

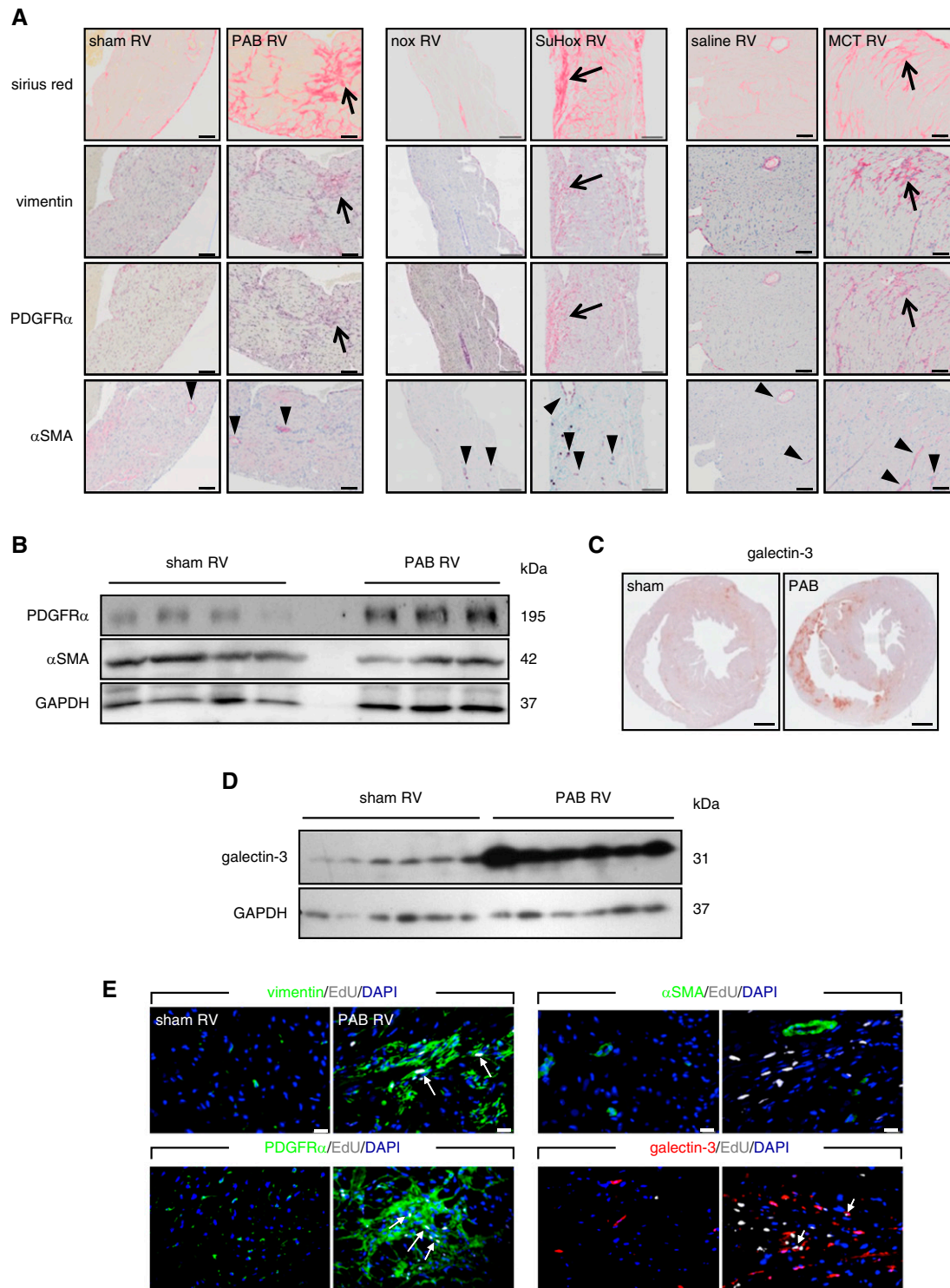


Figure 1. Right ventricle (RV) fibrosis is characterized by expansion of PDGFR α (platelet-derived growth factor receptor- α)-expressing cells. (A) Representative serial immunohistochemical staining of the RV fibrotic regions (Sirius red) against vimentin, PDGFR α , and α SMA (α -smooth muscle actin) from mice 21 days after pulmonary artery banding (PAB) (scale bars, 50 μ m), rats 6 weeks after Sugen5416 application (including 3-wk hypoxia exposure followed by 3-wk normoxia) (scale bars, 200 μ m), and rats 4 weeks after monocrotaline injection (scale bars, 100 μ m); $n = 4$ animals/group. Arrows mark the position of fibrotic region; arrowheads denote a coronary vessel. (B) Western blot detection of PDGFR α and α SMA protein expression in the RV; $n = 4$ –3 mice/group. (C) Representative immunohistochemical localization of galectin-3 expression in the murine hearts 3 weeks after PAB/sham (scale bars, 500 μ m). (D) Western blot detection of RV galectin-3 protein expression 3 weeks after PAB or sham; $n = 6$ mice/group. (E) Immunofluorescent detection of proliferation marker EdU in the RV fibrotic regions; $n = 4$ mice/group. MCT = monocrotaline; nox = normoxia; SuHox = Sugen5416/hypoxia.

In a prolonged PAB model, after 8 weeks there was no significant difference in fibrosis levels and main functional parameters in comparison with 3 weeks PAB (see Figures E6A–E6C). Similar to 3 weeks, at 8 weeks there was no significant correlation between fibrosis and functional parameters (see Figures E6D–E6F). An antifibrotic effect of NaLac and pirfenidone was not observed (see Figures E6G–E6I).

RV Fibrosis in Patients with IPAH Is Associated with Increased Galectin-3 Levels That Are Not Correlated with Functional Parameters

As potential RV fibrosis marker, we measured circulating galectin-3 levels in two independent cohorts of patients with PAH. Serum levels of galectin-3 were significantly increased in both derivation (Graz, $n = 10$) and validation (Baltimore, $n = 81$) PAH cohorts compared with donor samples, and showed no significant difference between IPAH and SSc-PAH subtypes (Figures 5A–5C). Galectin-3 gene and protein lung expression levels were comparable between donors and IPAH (Figures 5D and 5F). Similarly, there was no difference in galectin-3 expression between donors and IPAH in the isolated pulmonary arteries (Figures 5E and 5F). Galectin-3 was predominately localized to isolated, single cells in the adventitial layer of pulmonary arteries (Figure 5G). In the RV autopsy samples taken from patients with end-stage PAH, galectin-3 staining was observed in a subpopulation of cardiac fibroblasts and inflammatory cells (Figure 5H). Similar to results obtained from animal models, cardiac fibroblasts showed a staining pattern characterized by PDGFR α and vimentin immunoreactivity and lacking α SMA staining (Figure 5H). A comparable localization pattern of fibrotic markers was observed in RV biopsy samples taken from patients with dilated cardiomyopathy and pulmonary hypertension (see Figure E7A).

Furthermore, we observed a correlation of galectin-3 staining with the fibrosis score

(see Figure E7B). Cumulatively, our results indicated a predominantly cardiac source of increased circulating galectin-3 levels in patients with PAH. We therefore used serum galectin-3 levels to check for possible associations between RV fibrosis and function in patients with PAH. There was a weak correlation of galectin-3 serum levels only with cardiac output in patients with PAH (see Table E3). However, this correlation was caused by a strong correlation within the SSc-PAH subtype (see Table E3). Galectin-3 serum levels were not significantly correlated with mean pulmonary artery pressure, pulmonary vascular resistance, pulmonary artery wedge pressure, cardiac output or index, NT-proBNP (N-terminal pro-B-type natriuretic peptide), and 6-minute-walk distance in either of the IPAH cohorts (see Table E3).

Discussion

Both RV fibrosis and functional impairment have been reported in patients with PAH (5, 26), yet the functional consequences of RV fibrosis on RV function are unexplored and the cellular composition and molecular mechanisms that govern the fibrosis development have not been elucidated.

In the current study we identified the galectin-3-driven expansion of PDGFR α ⁺ cells as an important contributor to RV fibrosis development. Vimentin⁺/PDGFR α ⁺ cells represented the major fibroblast population with scant presence of α SMA-expressing fibroblasts (myofibroblasts) in RV fibrotic regions. This is similar to recent findings in the LV, where LV fibrotic regions were populated mainly by PDGFR α ⁺ cells, constituting a large subpopulation of cardiac resident collagen 1a1-expressing cells (14–16). Galectin-3 was partially colocalized with fibroblast markers. This suggests that fibroblasts produce galectin-3 as an autocrine mechanism. However, it could also be secreted by recruited inflammatory

cells and a recent study reported increased galectin-3 gene expression in peripheral blood cells from patients with IPAH (27). The exact cellular origin of punctuate extracellular galectin-3 deposits detected in RV fibrotic regions requires further investigation.

In agreement with our experimental models, we detected PDGFR α ⁺ and galectin-3⁺ cells in the RV from patients with PAH. The involvement of galectin-3 in RV fibrosis was substantiated in human RV samples showing a positive correlation between galectin-3 and fibrosis score and by our *in vivo* findings. Both genetic deletion (galectin-3 knockout mice) and the therapeutic approach (galectin-3 inhibitor) were associated with a significant amelioration of RV fibrosis, although some RV fibrosis remained, indicating the involvement of other mechanisms, such as PDGF (28) or TGF β -driven pathways (29). Activation of such alternative mechanisms could be responsible for the resistance to therapy in the chronic setting, as observed in our extended study at 8 weeks post-PAB.

The major finding of our study is the lack of significant RV functional improvement on fibrosis amelioration. This disconnect was independent of our intervention suggesting that pirfenidone did not use different pathologic mechanisms (30, 31) as compared with our alternative interventions. This is in contrast to an LV pressure overload model in which pirfenidone administration or galectin-3 inhibition ameliorated both LV fibrosis and dysfunction (31, 32). Another study showed no effect of galectin-3 inhibition on LV fibrosis and dysfunction, but rather on the hypertrophic myocardial response (33).

We observed the expected correlation of RV fibrosis with RV end diastolic pressure, cardiac output, and tricuspid annular plane systolic excursion in the pooled data from all experimental animals indicating that both fibrosis and RV dysfunction originate from the same pathologic mechanisms. However, this does not imply a causal relationship. Indeed, a

Figure 2. (Continued). RV fibrosis. (D) Representative immunohistochemical staining of the murine hearts against vimentin, PDGFR α (platelet-derived growth factor receptor- α), and galectin-3 ($n = 3$). Scale bars, 500 μ m. (E) Representative immunofluorescence staining of the RV fibrotic regions against vimentin, PDGFR α , α SMA (α -smooth muscle actin), and galectin-3 ($n = 2$). Arrows depict cells showing colocalization of PDGFR α and vimentin or galectin-3. Scale bars, 20 μ m. (F) Echocardiographic assessment of RV free wall thickness. Invasive hemodynamic measurement of (G) RV systolic pressure and (H) RV end diastolic pressure. Echocardiographic assessment of (I) cardiac output, (J) tricuspid annular plane systolic excursion, and (K) early peak of RV relaxation velocity. Two-way ANOVA with Bonferroni *post hoc* test, * $P < 0.05$. CO = cardiac output; e' = RV relaxation velocity; GAL3 KO = galectin-3 homozygous knockout mice; i.p. = intraperitoneal; NaLac = *N*-acetylglucosamine; PAB = pulmonary artery banding; RVEDP = RV end diastolic pressure; RVFW = RV free wall thickness; RVSP = RV systolic pressure; TAPSE = tricuspid annular plane systolic excursion; WT = wild type.

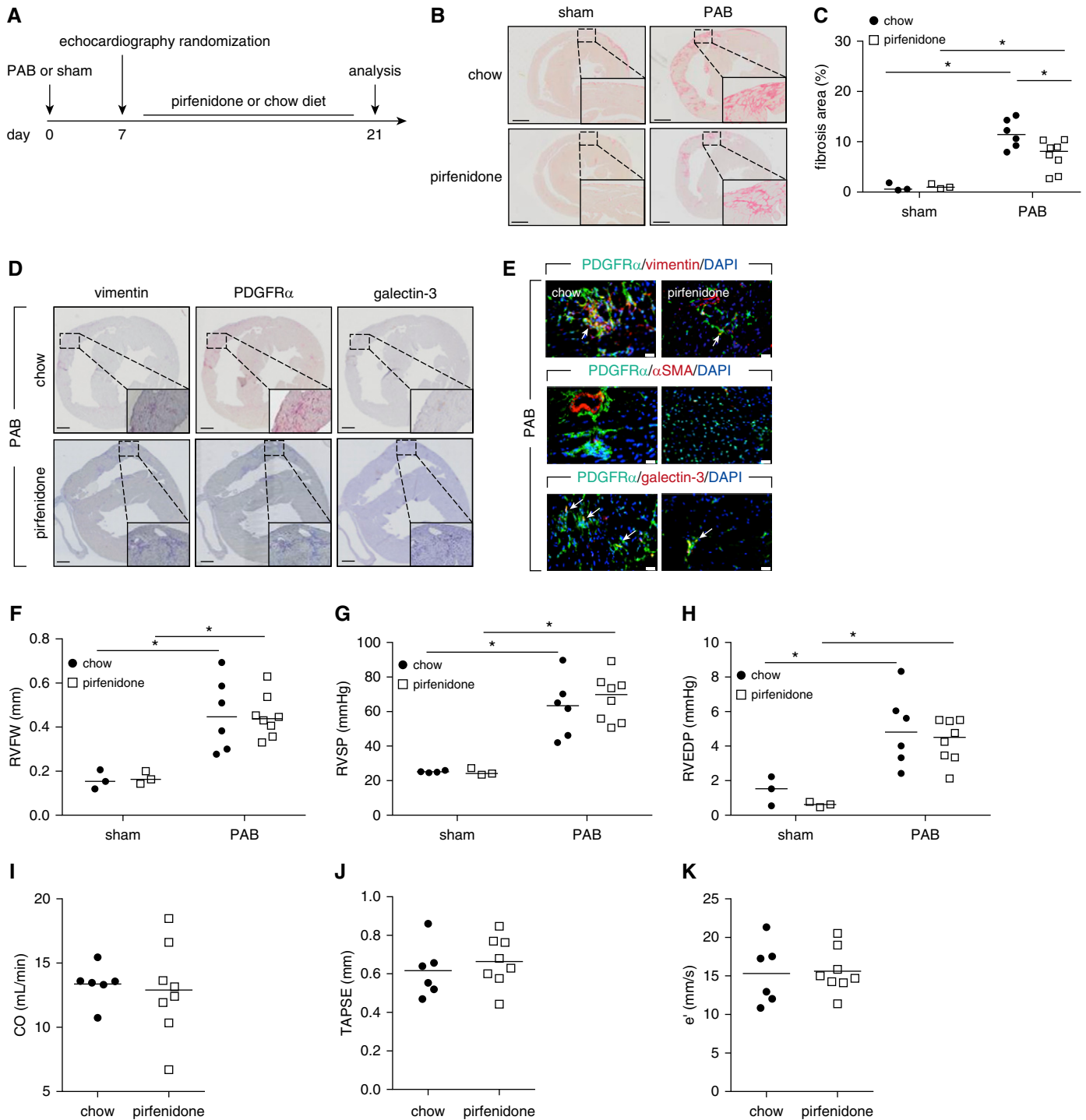


Figure 3. The antifibrotic agent pirfenidone ameliorates the progression of right ventricle (RV) fibrosis. **(A)** Schematic representation of the experimental setup. Hearts were collected from pirfenidone- or chow diet-treated mice 21 days after pulmonary artery banding or sham operation. **(B)** Representative Sirius red staining. Scale bars, 1 mm. **(C)** Quantification of RV fibrosis. **(D)** Representative immunohistochemical staining of the murine hearts against vimentin, PDGFR α (platelet-derived growth factor receptor- α), and galectin-3 ($n = 3$). Scale bars, 500 μm . **(E)** Representative immunofluorescence staining of the RV fibrotic regions against vimentin, PDGFR α , αSMA (α -smooth muscle actin), and galectin-3 ($n = 2$). Arrows depict cells showing colocalization of PDGFR α and vimentin or galectin-3. Scale bars, 20 μm . **(F)** Echocardiographic assessment of RV free wall thickness. Invasive hemodynamic measurement of **(G)** RV systolic pressure and **(H)** RV end diastolic pressure. Echocardiographic assessment of **(I)** cardiac output, **(J)** tricuspid annular plane systolic excursion, and **(K)** early peak of RV relaxation velocity. Two-way ANOVA with Bonferroni *post hoc* test, $*P < 0.05$. CO = cardiac output; e' = RV relaxation velocity; PAB = pulmonary artery banding; RVEDP = RV end diastolic pressure; RVFW = RV free wall thickness; RVSP = RV systolic pressure; TAPSE = tricuspid annular plane systolic excursion.

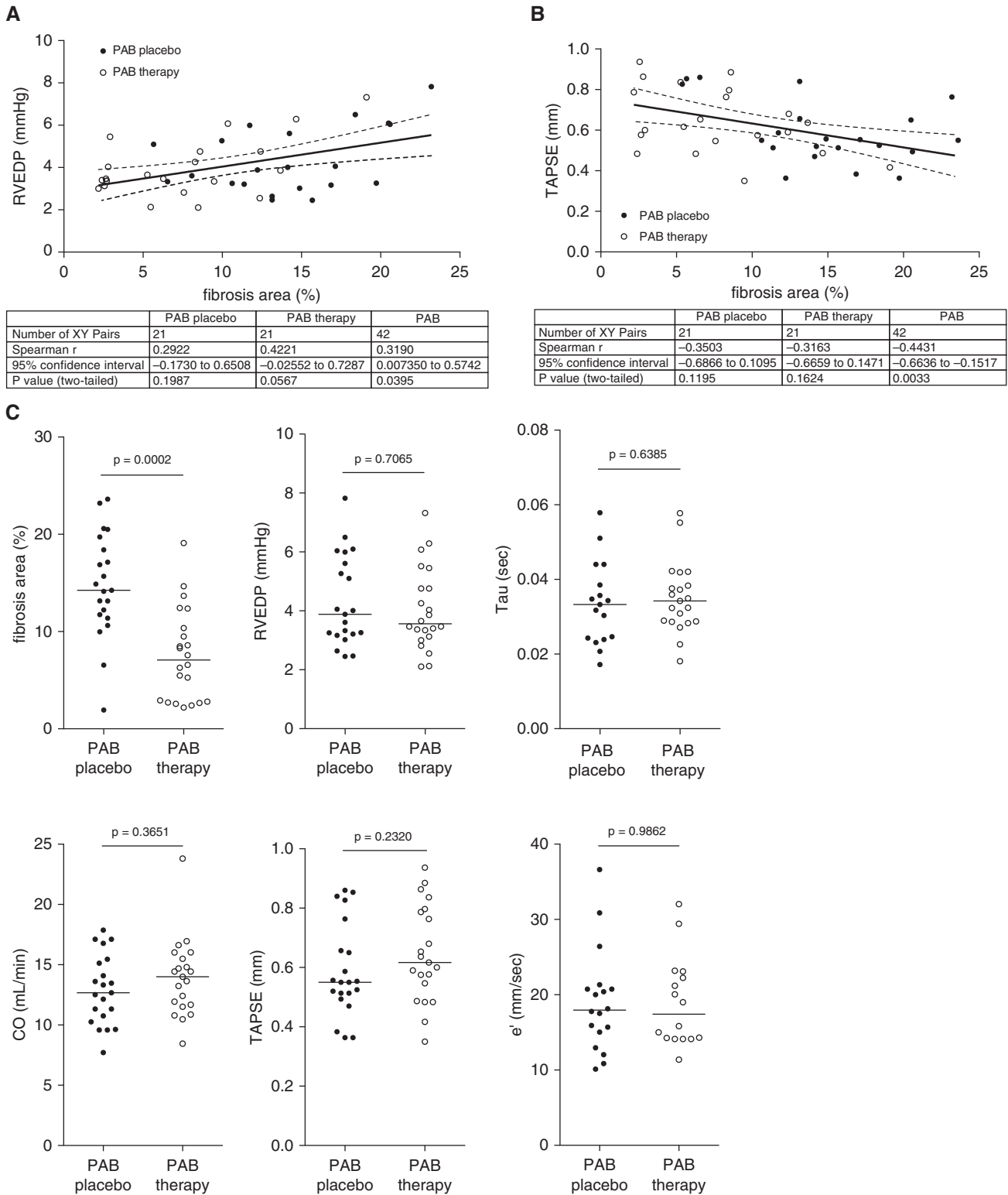


Figure 4. Disconnect between right ventricular (RV) fibrosis and function. Fibrosis and function were assessed 21 days after the pulmonary artery banding operation in control and treated mice (galectin-3 inhibitor *N*-acetylglucosamine, galectin-3 knock-out mice, pirfenidone). (A) Correlation of RV fibrosis with RV end diastolic pressure (RVEDP) (catheter derived), and (B) tricuspid annular plane systolic excursion (TAPSE) (echo-derived). Mann-Whitney test and nonparametric correlation (Spearman). Linear regression (full line) with 95% confidence intervals (dashed lines). (C) Pooled data representing RV fibrosis area, RVEDP, tau (time constant of monoexponential curve fitting model of RV diastolic pressure decay), cardiac output, TAPSE, and RV relaxation velocity. CO = cardiac output; e' = RV relaxation velocity; PAB = pulmonary artery banding.

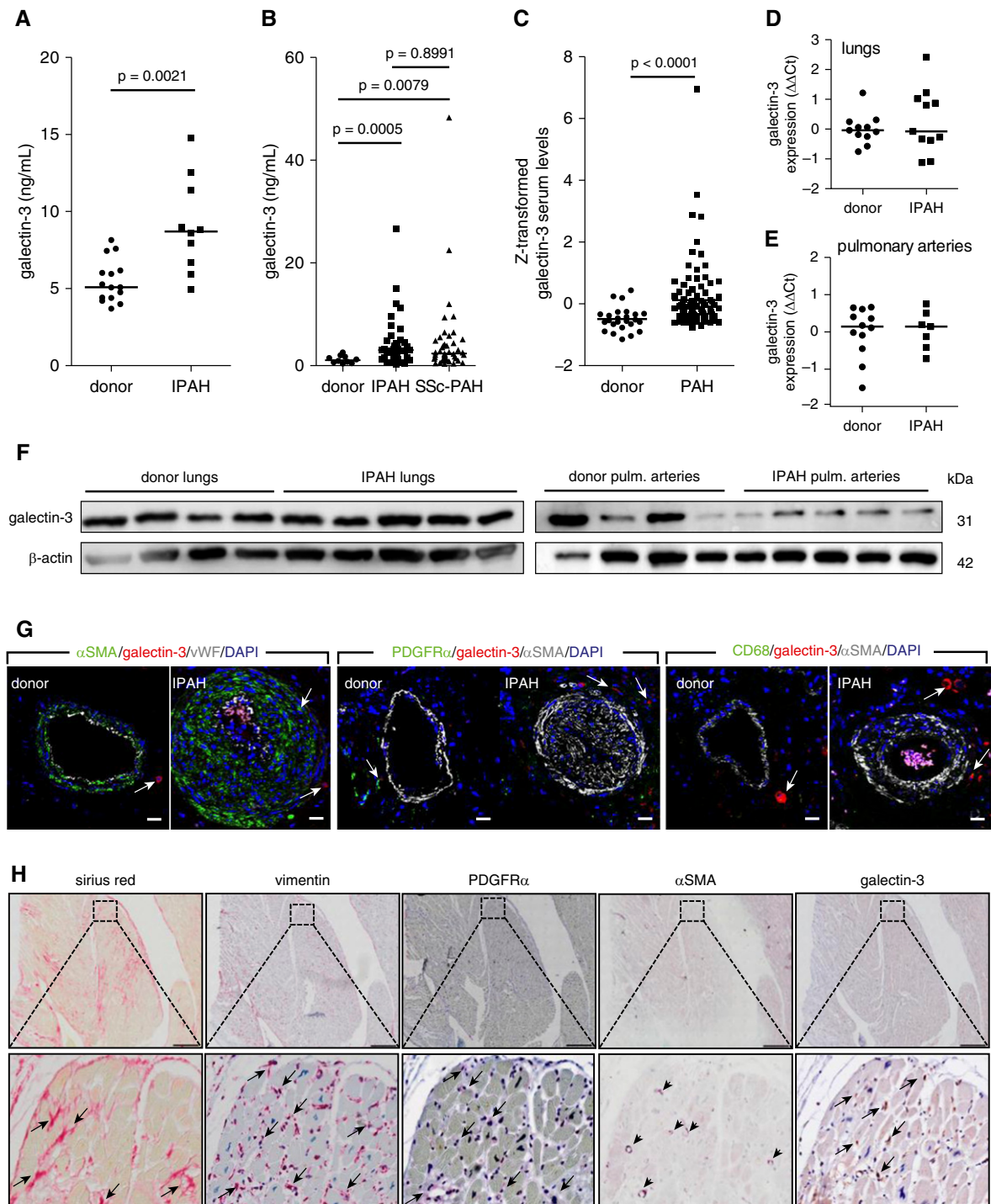


Figure 5. Galectin-3 is expressed in the human right ventricle (RV) and serum levels are elevated in patients with pulmonary arterial hypertension (PAH). ELISA measurement of serum galectin-3 levels in (A) Graz ($n = 10$) and (B) Baltimore cohorts ($n = 81$ total; IPAH = 38; systemic sclerosis PAH = 43). (C) Z-transformed serum galectin-3 levels in combined cohorts donor ($n = 25$) and PAH ($n = 91$). Student's *t* test with Welch correction. Quantitative PCR determination of galectin-3 mRNA expression in (D) lung homogenates and (E) isolated pulmonary arteries. (F) Protein expression of galectin-3 in lung homogenates and isolated pulmonary arteries. (G) Representative immunofluorescent colocalization of galectin-3 with smooth muscle (α SMA [α -smooth muscle actin]), endothelial (von Willebrand factor), fibroblast (PDGFR α [platelet-derived growth factor receptor- α]), and macrophage markers (CD68) in human pulmonary arteries. Scale bars, 20 μ m. (H) Immunohistochemical staining of the RV against vimentin, PDGFR α , α SMA, and galectin-3 on RV autopsy samples from a patient with idiopathic PAH. Fibrotic regions were detected using Sirius red stain. Arrows depict positively stained regions/cells; arrowheads mark cardiac vessels. Scale bars, 500 μ m (50 μ m in magnified regions). IPAH = idiopathic pulmonary arterial hypertension; SSc-PAH = systemic sclerosis pulmonary arterial hypertension; vWF = von Willebrand factor.

recent study found that sarcomere impairment of the cardiomyocytes explains most of the RV dysfunction in scleroderma patients with PAH (34). This agrees with previous investigations showing dysfunctional RV sarcomeres from patients with PAH and the rat PAB model (5, 35).

Complementing our data from the human RV tissue, we detected increased circulating levels of galectin-3 in patients with PAH. However, we found no increase in galectin-3 expression in the lungs from patients with IPAH, in contrast to a very recent study (36). Our findings imply that the increased galectin-3 serum levels are not associated with the remodeling process in the pulmonary arteries, but with fibrosis development in the heart. Furthermore, we did not observe a significant correlation of galectin-3 serum levels with cardiac index or NT-proBNP either in the separate or the combined cohort of 48 patients with IPAH, opposing an earlier study investigating galectin-3 and RV systolic and diastolic function parameters in 12 patients with IPAH (12). Moreover, in larger cohorts investigating patients with LV disease, galectin-3 levels were also independent of NT-proBNP (37).

A recent study observed no correlations between circulating galectin-3 and ventricular fibrosis and inflammation in patients with LV heart failure (38), although this was correlated with myocardial galectin-3 levels. This suggests that the LV might differ in this respect from the RV.

We have limited our study to cardiac fibroblasts, but such processes as adaptive angiogenesis and loss of capillaries could have a significant impact on RV function (39). In our study the diminished capillary density was not improved with the tested antifibrotic treatments suggesting a potential role of endothelial cells in RV dysfunction development, potentially via promotion of myocardial ischemia. Endothelial cells could also have a more direct role in fibrosis development through the process of endothelial-to-mesenchymal transition (40), although this transdifferentiation process has recently been questioned in the adult ventricle (15, 41). Additional studies are needed to address the distinct roles of endothelial cells and, more broadly, the vascular compartment in RV dysfunction.

Our study was limited by the use of a single animal model that only partially addresses the human disease. Another limiting factor was the lack of reliable

methods to noninvasively quantify ventricular fibrosis in patients. This technical limitation precluded direct correlation of RV fibrosis with functional in patients with PAH. Although in IPAH and SSc-PAH circulating galectin-3 levels were increased, only in patients with SSc-PAH were they inversely correlated with cardiac output. This could be caused by a different extent or mechanism of RV fibrosis in SSc-PAH compared with IPAH (42); however, it seems likely that the cardiomyocyte impairment could be the main cause for the observed differences (34).

Cumulatively, our findings suggest that galectin-3 contributes to RV fibrosis development under pressure overload conditions. However, mechanisms other than fibrosis may decide on RV functional impairment. Thus, a combination therapy that targets different pathways might be needed to achieve a meaningful clinical impact. ■

Author disclosures are available with the text of this article at www.atsjournals.org.

Acknowledgment: The authors appreciate the excellent technical support of Julia Schittl, Sanja Kozaj, Thomas Fuchs, and Alexandra Treitler.

References

- Brewis MJ, Bellofiore A, Vanderpool RR, Chesler NC, Johnson MK, Naeije R, *et al*. Imaging right ventricular function to predict outcome in pulmonary arterial hypertension. *Int J Cardiol* 2016;218:206–211.
- van de Veerdonk MC, Kind T, Marcus JT, Mauritz GJ, Heymans MW, Bogaard HJ, *et al*. Progressive right ventricular dysfunction in patients with pulmonary arterial hypertension responding to therapy. *J Am Coll Cardiol* 2011;58:2511–2519.
- Bogaard HJ, Natarajan R, Henderson SC, Long CS, Kraskauskas D, Smithson L, *et al*. Chronic pulmonary artery pressure elevation is insufficient to explain right heart failure. *Circulation* 2009;120:1951–1960.
- Paulin R, Sutendra G, Gurtu V, Dromparis P, Haromy A, Provencher S, *et al*. A miR-208-Mef2 axis drives the decompensation of right ventricular function in pulmonary hypertension. *Circ Res* 2015;116:56–69.
- Rain S, Handoko ML, Trip P, Gan CT, Westerhof N, Stienen GJ, *et al*. Right ventricular diastolic impairment in patients with pulmonary arterial hypertension. *Circulation* 2013;128:2016–2025.
- Nagendran J, Sutendra G, Paterson I, Champion HC, Webster L, Chiu B, *et al*. Endothelin axis is upregulated in human and rat right ventricular hypertrophy. *Circ Res* 2013;112:347–354.
- Gomez-Arroyo J, Sakagami M, Syed AA, Farkas L, Van Tassel B, Kraskauskas D, *et al*. Ilprost reverses established fibrosis in experimental right ventricular failure. *Eur Respir J* 2015;45:449–462.
- Tanaka Y, Takase B, Yao T, Ishihara M. Right ventricular electrical remodeling and arrhythmogenic substrate in rat pulmonary hypertension. *Am J Respir Cell Mol Biol* 2013;49:426–436.
- Egemnazarov B, Crnkovic S, Nagy BM, Olschewski H, Kwapiszewska G. Right ventricular fibrosis and dysfunction: actual concepts and common misconceptions. *Matrix Biol* 2018;68–69:507–521.
- van der Velde AR, Meijers WC, Ho JE, Brouwers FP, Rienstra M, Bakker SJ, *et al*. Serial galectin-3 and future cardiovascular disease in the general population. *Heart* 2016;102:1134–1141.
- van der Velde AR, Gullestad L, Ueland T, Aukrust P, Guo Y, Adourian A, *et al*. Prognostic value of changes in galectin-3 levels over time in patients with heart failure: data from CORONA and COACH. *Circ Heart Fail* 2013;6:219–226.
- Fenster BE, Lasalvia L, Schroeder JD, Smyser J, Silveira LJ, Buckner JK, *et al*. Galectin-3 levels are associated with right ventricular functional and morphologic changes in pulmonary arterial hypertension. *Heart Vessels* 2016;31:939–946.
- Calvier L, Legchenko E, Grimm L, Sallmon H, Hatch A, Plouffe BD, *et al*. Galectin-3 and aldosterone as potential tandem biomarkers in pulmonary arterial hypertension. *Heart* 2016;102:390–396.
- Ali SR, Ranjbarvaziri S, Talkhabi M, Zhao P, Subat A, Hojjat A, *et al*. Developmental heterogeneity of cardiac fibroblasts does not predict pathological proliferation and activation. *Circ Res* 2014;115:625–635.
- Moore-Morris T, Guimarães-Camboá N, Banerjee I, Zambon AC, Kisseleva T, Velayoudon A, *et al*. Resident fibroblast lineages mediate pressure overload-induced cardiac fibrosis. *J Clin Invest* 2014;124:2921–2934.
- Pinto AR, Ilinykh A, Ivey MJ, Kuwabara JT, D'Antoni ML, Debuque R, *et al*. Revisiting cardiac cellular composition. *Circ Res* 2016;118:400–409.
- Moore-Morris T, Cattaneo P, Puceat M, Evans SM. Origins of cardiac fibroblasts. *J Mol Cell Cardiol* 2016;91:1–5.
- Skelly DA, Squiers GT, McLellan MA, Bolisetty MT, Robson P, Rosenthal NA, *et al*. Single-cell transcriptional profiling reveals cellular diversity and intercommunication in the mouse heart. *Cell Reports* 2018;22:600–610.

19. Atsina K, Tedford RJ, Valera L, Housten T, Mathai SC, Kolb TM, *et al*. Serum galectin-3 is elevated in group I pulmonary arterial hypertension and is associated with unfavorable hemodynamics [abstract]. *Am J Respir Cell Mol Biol* 2014;189:A3866.
20. Crnkovic S, Egemnazarov B, Kovacs G, Marsh L, Ghanim B, Klepetko W, *et al*. Increased galectin-3 levels in pulmonary hypertension mediate right ventricle fibrotic response [abstract]. *Am J Respir Cell Mol Biol* 2015;191:A1040.
21. Egemnazarov B, Schmidt A, Crnkovic S, Sydykov A, Nagy BM, Kovacs G, *et al*. Pressure overload creates right ventricular diastolic dysfunction in a mouse model: assessment by echocardiography. *J Am Soc Echocardiogr* 2015;28:828–843.
22. Sörme P, Qian Y, Nyholm PG, Leffler H, Nilsson UJ. Low micromolar inhibitors of galectin-3 based on 3'-derivatization of N-acetyllactosamine. *ChemBioChem* 2002;3:183–189.
23. Kwapiszewska G, Wygrecka M, Marsh LM, Schmitt S, Trösser R, Wilhelm J, *et al*. Fhl-1, a new key protein in pulmonary hypertension. *Circulation* 2008;118:1183–1194.
24. Crnkovic S, Schmidt A, Egemnazarov B, Wilhelm J, Marsh LM, Ghanim B, *et al*. Functional and molecular factors associated with TAPSE in hypoxic pulmonary hypertension. *Am J Physiol Lung Cell Mol Physiol* 2016;311:L59–L73.
25. Kojonazarov B, Sydykov A, Pullamsetti SS, Luitel H, Dahal BK, Kosanovic D, *et al*. Effects of multikinase inhibitors on pressure overload-induced right ventricular remodeling. *Int J Cardiol* 2013;167:2630–2637.
26. Venalis P, Kumánovics G, Schulze-Koops H, Distler A, Dees C, Zerr P, *et al*. Cardiomyopathy in murine models of systemic sclerosis. *Arthritis Rheumatol* 2015;67:508–516.
27. Chesné J, Danger R, Botturi K, Reynaud-Gaubert M, Mussot S, Stern M, *et al*.; COLT Consortium. Systematic analysis of blood cell transcriptome in end-stage chronic respiratory diseases. *PLoS One* 2014;9:e109291.
28. Pontén A, Folestad EB, Pietras K, Eriksson U. Platelet-derived growth factor D induces cardiac fibrosis and proliferation of vascular smooth muscle cells in heart-specific transgenic mice. *Circ Res* 2005;97:1036–1045.
29. Koitabashi N, Danner T, Zaiman AL, Pinto YM, Rowell J, Mankowski J, *et al*. Pivotal role of cardiomyocyte TGF- β signaling in the murine pathological response to sustained pressure overload. *J Clin Invest* 2011;121:2301–2312.
30. Yamagami K, Oka T, Wang Q, Ishizu T, Lee JK, Miwa K, *et al*. Pirfenidone exhibits cardioprotective effects by regulating myocardial fibrosis and vascular permeability in pressure-overloaded hearts. *Am J Physiol Heart Circ Physiol* 2015;309:H512–H522.
31. Wang Y, Wu Y, Chen J, Zhao S, Li H. Pirfenidone attenuates cardiac fibrosis in a mouse model of TAC-induced left ventricular remodeling by suppressing NLRP3 inflammasome formation. *Cardiology* 2013;126:1–11.
32. Yu L, Ruifrok WP, Meissner M, Bos EM, van Goor H, Sanjabi B, *et al*. Genetic and pharmacological inhibition of galectin-3 prevents cardiac remodeling by interfering with myocardial fibrogenesis. *Circ Heart Fail* 2013;6:107–117.
33. Frunza O, Russo I, Saxena A, Shinde AV, Humeres C, Hanif W, *et al*. Myocardial galectin-3 expression is associated with remodeling of the pressure-overloaded heart and may delay the hypertrophic response without affecting survival, dysfunction, and cardiac fibrosis. *Am J Pathol* 2016;186:1114–1127.
34. Hsu S, Kokkonen-Simon KM, Kirk JA, Kolb TM, Damico RL, Mathai SC, *et al*. Right ventricular myofilament functional differences in humans with systemic sclerosis-associated versus idiopathic pulmonary arterial hypertension. *Circulation* 2018;137:2360–2370.
35. Rain S, Andersen S, Najafi A, Gammelgaard Schultz J, da Silva Gonçalves Bós D, Handoko ML, *et al*. Right ventricular myocardial stiffness in experimental pulmonary arterial hypertension: relative contribution of fibrosis and myofibril stiffness. *Circ Heart Fail* 2016;9:e002636.
36. Barman SA, Chen F, Li X, Haigh S, Stepp DW, Kondrikov D, *et al*. Galectin-3 promotes vascular remodeling and contributes to pulmonary hypertension. *Am J Respir Crit Care Med* 2018;197:1488–1492.
37. Lok DJ, Van Der Meer P, de la Porte PW, Lipsic E, Van Wijngaarden J, Hillege HL, *et al*. Prognostic value of galectin-3, a novel marker of fibrosis, in patients with chronic heart failure: data from the DEAL-HF study. *Clin Res Cardiol* 2010;99:323–328.
38. Besler C, Lang D, Urban D, Rommel KP, von Roeder M, Fengler K, *et al*. Plasma and cardiac galectin-3 in patients with heart failure reflects both inflammation and fibrosis: implications for its use as a biomarker. *Circ Heart Fail* 2017;10:e003804.
39. Kolb TM, Peabody J, Baddoura P, Fallica J, Mock JR, Singer BD, *et al*. Right ventricular angiogenesis is an early adaptive response to chronic hypoxia-induced pulmonary hypertension. *Microcirculation* 2015;22:724–736.
40. Zeisberg EM, Tarnavski O, Zeisberg M, Dorfman AL, McMullen JR, Gustafsson E, *et al*. Endothelial-to-mesenchymal transition contributes to cardiac fibrosis. *Nat Med* 2007;13:952–961.
41. He L, Huang X, Kanisicak O, Li Y, Wang Y, Li Y, *et al*. Preexisting endothelial cells mediate cardiac neovascularization after injury. *J Clin Invest* 2017;127:2968–2981.
42. Overbeek MJ, Mouchaers KT, Niessen HM, Hadi AM, Kupreishvili K, Boonstra A, *et al*. Characteristics of interstitial fibrosis and inflammatory cell infiltration in right ventricles of systemic sclerosis-associated pulmonary arterial hypertension. *Int J Rheumatol* 2010;2010:604615.